SCIENTIFIC REPORTS

OPEN

SUBJECT AREAS:
SYNTHESIS AND PROCESSING
NANOWIRES

Received
4 September 2013

Accepted
1 October 2013

Published
16 October 2013

Correspondence and requests for materials should be addressed to X.-F.L. (xflu@jlu.edu.cn) or C.W. (cwang@jlu.edu.cn)

A facile strategy to decorate Cu_9S_5 nanocrystals on polyaniline nanowires and their synergetic catalytic properties

Xiao-feng Lu, Xiu-jie Bian, Zhi-cheng Li, Dan-ming Chao & Ce Wang

Alan G. MacDiarmid Institute, College of Chemistry, Jilin University, Changchun 130012 PR China.

Here, we demonstrated a novel method to decorate Cu_9S_5 nanocrystals on polyaniline (PANI) nanowires using the dopant of mercaptoacetic acid (MAA) in the PANI matrix as the sulfur source under a hydrothermal reaction. TEM images showed that Cu_9S_5 nanocrystals with a size in the range of 5–20 nm were uniformly formed on the surface of PANI nanowires. Significantly, the as-prepared PANI/Cu_9S_5 composite nanowires have been proven to be novel peroxidase mimics toward the oxidation of the peroxidase substrate 3,3′,5,5′-tetramethylbenzidine (TMB) in the presence of H_2O_2. Due to the synergetic effects between polyaniline nanowires and Cu_9S_5 nanocrystals, the obtained PANI/Cu_9S_5 composite nanowires exhibit superior catalytic activity over the independent components. This work not only presents a simple and versatile method to decorate semiconductor nanocrystals on the surface of conducting polymer nanostructures, but also provides fundamental guidelines for further investigations into the synergetic effect between conducting polymers and other materials.

Over the past few decades, artificial enzyme mimics have generated great interest because of their improved properties relative to natural enzymes, such as easy and low costs of preparation, purification and storage, greater resistance to extremes of acidity, temperature and inhibitors[1–3]. Indeed, many enzyme mimics such as hemin, hematin, hemoglobin, cyclodextrin, porphyrin etc. have been developed and applied in the fields of clinical diagnosis, environmental science and biotechnology[4–12]. At present, the synthesis and application of nanomaterials in the field of catalysis has become an active field of scientific research because of their large surface area, high catalytic activity and good selectivity, and some nanomaterials have been found to possess enzyme mimetic activity[13]. For example, Fe_3O_4 magnetic nanoparticles were first reported to process intrinsic peroxidase-like activity, which could be used to detect H_2O_2 and thrombin[14–16]. The nanomaterials as artificial enzyme mimics take the advantages of low cost, easy preparation, high activity and good stability. In the past few years, various kinds of nanomaterials have been explored as enzymatic mimics, including metal oxide nanoparticles (NPs) and nanowires (such as Fe_3O_4 NPs, Co_3O_4 NPs, CuO NPs, CeO_2 NPs, V_2O_5 nanowires)[14,17–20], metal-based nanomaterials (such as Au NPs, bimetallic alloy NPs, bimetallic hybrid nanorods)[21–24], carbon nanomaterials (such as graphene oxide, carbon nanotubes, carbon nanodots)[25–27], chalcogenide nanomaterials (such as FeS, FeSe, CuS, CdS NPs)[28–31], multiferroic nanomaterials (such as $BiFeO_3$ NPs, $CoFe_2O_4$ NPs)[32,33], and even coordination polymer NPs[34] or carboxyl functionalized mesoporous polymer[35].

During the process of catalytic reactions, the interfaces play an important role, which could result in a better activity and selectivity[36]. Recently, Yang and co-workers designed multiple metal-metal oxide interfaces to study the catalysis of sequential reactions[37]. It was found that two different kinds of metal-metal oxide interfaces could catalyze two distinct sequential reactions. Therefore, the fabrication of composite nanomaterials with well-defined composition and interfaces has been extensively studied to enhance or extend the functionality of each component. A variety of graphene or carbon nanotube based nanomaterials have been explored with peroxidase-like catalytic activity[38–41]. Typically, the Au NPs/graphene composite nanosheets process an enhanced catalytic activity in comparison to the independent Au-NPs and graphene, which could be due to the synergetic effect at their interfaces[41]. However, such synergetic effect has few been observed in other systems except the carbon based nanomaterials. In this study, we have shown for the first time that conducting polyaniline (PANI)/Cu_9S_5 composite nanowires showed a superior catalytic activity as artificial enzyme mimics compared to the independent polyaniline and Cu_9S_5 nanocomponents due to their synergetic effect.

PANI is one kind of conducting polymers that has been extensively studied in the past few decades. Compared to other intrinsic conducting polymers, the doping level of PANI can be simply controlled by a reversible acid/

base doping/dedoping process[42]. In recent years, PANI nanomaterials have attracted much attention because of their unique physical and chemical properties such as large surface area and high conductivity. Especially, one-dimensional PANI nanostructures such as nanofibers, nanorods and nanowires have become a focus subject in the field of conducting polymer nanotechnology because they process the advantages of both excellent conductivity and low-dimensional systems[43]. On the other hand, nanocomposites with PANI and inorganic nanomaterials showed improved electrical, thermal and optical properties due to the combined effect of the two components[44]. For the PANI based nanocomposites, the interactions between PANI and the inorganic nanomaterials are very vital to produce cooperatively enhanced performances. In the past few years, a series of PANI/sulfide nanocomposites have been fabricated for optic, optoelectronic and photoelectrochemcial applications[45–47]. However, it is still a great challenge to prepare low dimensional PANI nanocomposites with strong interactions between PANI and another inorganic nanocomponent to generate synergetic effect, which achieve an enhanced performance of the nanocomposites.

Herein, we have developed a novel method to fabricate PANI/Cu_9S_5 composite nanowires using the dopant of mercaptoacetic acid (MAA) in the PANI matrix as the sulfur source under a hydrothermal reaction. During the process of the reaction, the Cu_9S_5 nanocrystals could be in-situ formed on the surface of PNAI nanowires with strong interactions because the sulfur source of MAA was interacted with PANI nanowires through ionic bonds. Furthermore, it was found that the as-prepared PANI/Cu_9S_5 composite nanowires exhibited an enhanced catalytic activity toward the oxidation of 3,3′,5,5′-tetramethylbenzidine (TMB) in the presence of H_2O_2 over the independent PANI and Cu_9S_5 nanocomponents due to the synergetic effect between them.

Results

In this study, PANI/Cu_9S_5 composite nanowires were prepared by mixing MAA doped PANI nanowires and $CuCl_2 \cdot 2H_2O$ under a hydrothermal reaction. The synthetic strategy mainly involves three steps: (1) PANI nanowires doped with HCl was synthesized through a rapid-mixing method. (2) After treated by $NH_3 \cdot H_2O$, the dedoped PANI nanowires were again doped with MAA to form MAA doped PANI nanowires. (3) Mixing MAA doped PANI nanowires with copper ions under a hydrothermal condition to form PANI/Cu_9S_5 composite nanowires. During the reaction, the Cu_9S_5 nanocrystals were in-situ formed on the surface of PANI nanowires (Figure 1a). Figure 1b shows the TEM image of HCl doped PANI nanowires. It can be seen that the diameter of the PANI nanowires is in the range of 50–100 nm with a relatively smooth surface. After dedoping with $NH_3 \cdot H_2O$ and again doping with MAA, the size of nanowires did not change much, but showed a little aggregation (Figure S1 and 1c). After hydrothermal reaction, it can be clearly seen that Cu_9S_5 nanocrystals with a size in the range of 5–20 nm were uniformly formed on the surface of PANI nanowires (Figure 1d). A high resolution TEM (HRTEM) image exhibits that the as-prepared Cu_9S_5 nanocrystals showed a good crystallinity, with the lattice spacing of 0.20 nm which could be corresponding to the {0120} facet of Cu_9S_5[48] (Figure 1e). A control experiment was also performed to synthesize pristine Cu_9S_5 nanocrystals, which exhibit a particle or rod shape with a size of about 20–80 nm (Figure S2). This result indicates that the presence of PANI nanowires make for the Cu_9S_5 nanocrystals with a smaller size, which should be due to the strong interactions between the dopant of MAA and PANI nanowires during the hydrothermal reaction.

The formation of Cu_9S_5 nanocrystals on the surface of PANI nanowires were characterized by XRD measurement. Figure 2a shows the XRD patterns of the as-prepared PANI/Cu_9S_5 composite nanowires and Cu_9S_5 nanocrystals alone. From Figure 2a (red line), the diffraction peaks at $2\theta = 27.8^\circ$, 29.5°, 32.2°, 37.6°, 42.0°, 46.3°, 48.8°, 54.7° are indexed to the (0015), (107), (1010), (0114), (0117), (0120), (119), (1115) planes of Cu_9S_5, which is in good agreement with the Rhomb-centered structure (JCPDS 47-1748). Moreover, most of the strong diffraction peaks including (0015), (1010),

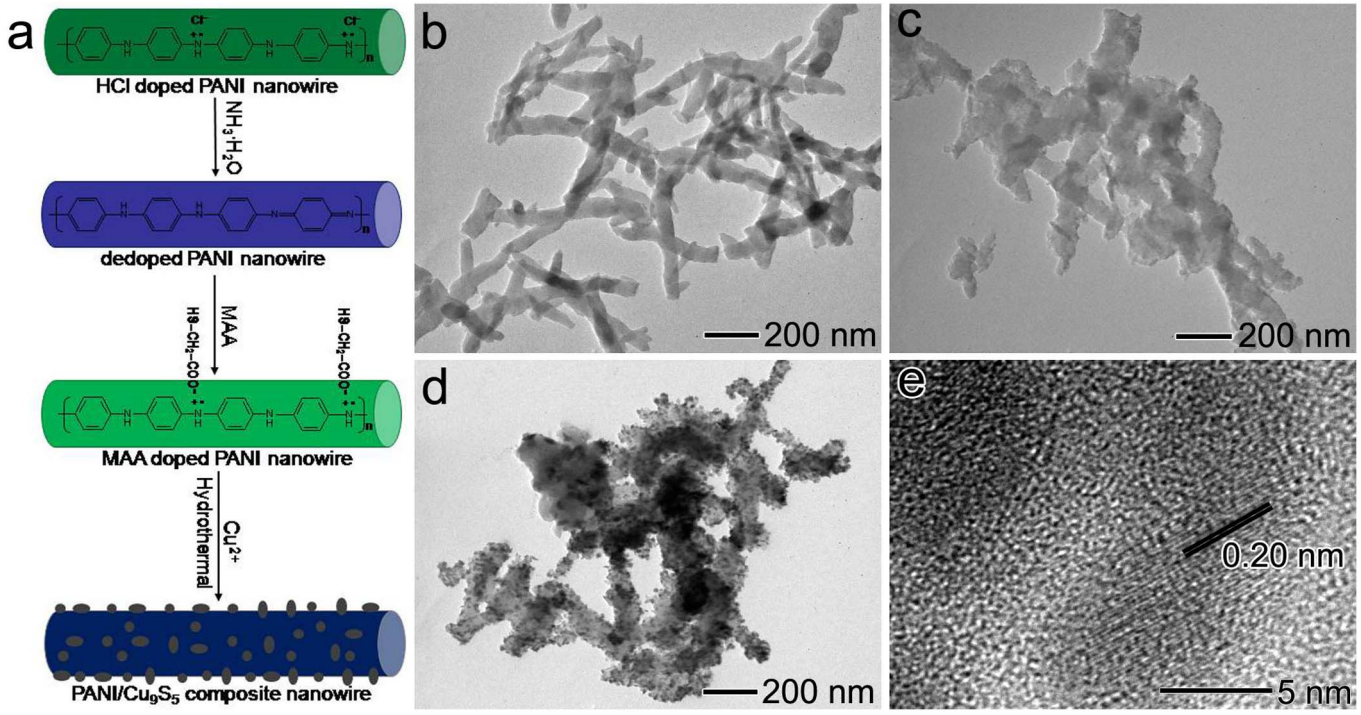

Figure 1 | Fabrication and morphology of the PANI/Cu_9S_5 composite nanowires. (a) Schematic illustration of the fabrication process to synthesize PANI/Cu_9S_5 composite nanowires. TEM images of the as-prepared (b) HCl doped PANI nanowires, (c) MAA doped PANI nanowires and (d) PANI/Cu_9S_5 composite nanowires. (e) HRTEM image of the as-prepared PANI/Cu_9S_5 composite nanowires.

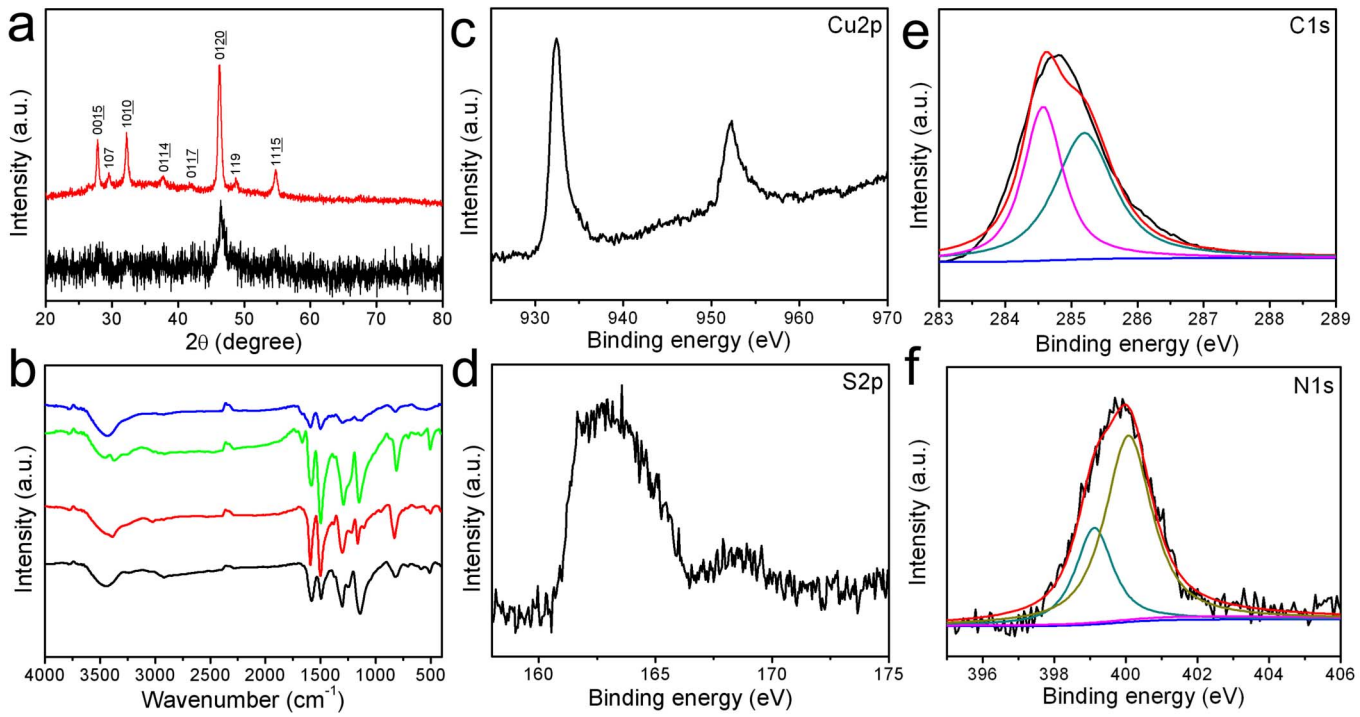

Figure 2 | Surface composition of the PANI/Cu_9S_5 composite nanowires. (a) XRD patterns of pristine Cu_9S_5 nanocrystals (red) and the as-prepared PANI/Cu_9S_5 composite nanowires (black). (b) FTIR spectra of HCl doped PANI nanowires (black), dedoped PANI nanowires with $NH_3 \cdot H_2O$ (red), MAA doped PANI nanowires (green) and PANI/Cu_9S_5 composite nanowires (blue). XPS spectra of the as-synthesized PANI/Cu_9S_5 composite nanowires: (c) Cu2p, (d) S2p, (e) C1s and (f) N1s.

(0120), (1115) have also been observed in the pattern of the as-prepared PANI/Cu_9S_5 composite nanowires, indicating the formation of Cu_9S_5 nanocrystals on the surface of PANI nanowires. We also estimated the size of Cu_9S_5 nanocrystals in accordance with the Scherrer's equation, and the average particle size of the Cu_9S_5 nanocrystals was calculated to be about 7.5 nm, which is consistent with the results originated from the TEM images.

Figure 2b shows the FTIR spectra of HCl doped PANI nanowires, dedoped PANI nanowires, MAA doped PANI nanowires and PANI/Cu_9S_5 composite nanowires, respectively. It was found that the characteristic peaks at 1581, 1495, 1304, 1244, 1142, 821 cm^{-1} which are corresponding to C=C stretching of the quinonoid and benzenoid rings, C-N and C=N stretching vibrations, N=Q=N (where Q denotes the quinonoid ring) bending vibration and the in-plane bending of C-H, respectively, were clearly observed for HCl doped PANI nanowires[45]. After dedoping by aqueous ammonia, the characteristic peaks of C=C stretching of the quinonoid and benzenoid rings shift to 1591 and 1500 cm^{-1}. And these two peaks shift to 1581 and 1498 cm^{-1} after doping with MAA. And a new peak at 1664 cm^{-1} appears for the MAA doped PANI nanowires, which is corresponding to the C=O stretching vibrations of MAA dopant. For PANI/Cu_9S_5 composite nanowires, the characteristic peaks were observed at 1591, 1500, 1300, 1130 and 822 cm^{-1}, indicating that the strong interactions between PANI nanowires and Cu_9S_5 nanocrystals.

Insight information of the surface chemical composition of the as-prepared PANI/Cu_9S_5 composite nanowires has been characterized by XPS analysis. As shown in Figure 2c, two strong peaks at 932.4 and 952.3 eV for Cu $2p_{3/2}$ and Cu $2p_{1/2}$, respectively, were clearly observed. The binding energy for Cu $2p_{3/2}$ in the Cu(2p) core level spectrum is close to the previous report of Cu^{+}[49]. In addition, a weak broad peak at about 945.0 eV are also observed, which could be attributed to the Cu^{2+}[50]. These results suggested that both Cu^{+} and Cu^{2+} ions existed in the PANI/Cu_9S_5 composite nanowires. Figure 2d shows the S 2p spectrum of PANI/Cu_9S_5 composite nanowires. The binding energy of S 2p appears at about 162.9 eV, which is generally attributed to the formation of Cu-S bond. And another weak peak centered at about 168.7 eV could be ascribed to the oxidized sulfur species such as sulfonate[51]. On the other hand, the C 1s of PANI in PANI/Cu_9S_5 composite nanowires has also been detected and could be deconvoluted into two components (Figure 2e). The peak at about 284.6 eV is attributed to C-C bond, while the other peak at about 285.2 eV is related to C-N bond. Similarly, the N1s spectrum could also be deconvoluted into two components, with binding energy at 400.1 and 399.1 eV, respectively (Figure 2f). The former peak is attributed to neutral nitrogen moieties in PANI[52]. The later signal at 399.1 eV is usually ascribed to uncharged deprotonated imine (=N-) atoms[52]. This result indicated that the doping degree was low in the PANI/Cu_9S_5 composite nanowires.

The formation of the MAA doped PANI nanowires and PANI/Cu_9S_5 composite nanowires has been proved by UV-vis absorption spectra. As shown in Figure 3a, HCl doped PANI nanowires exhibited characteristic color in green. After dedoping by ammonia water, the color turned to blue. Then it became back to light green after again doping with MAA. This result indicated that MAA had been doped in the PANI chains. The UV-vis absorption spectrum of the HCl doped PANI nanowires showed three characteristic absorption bands at around 360, 425 and $>$ 800 nm (Figure 3b). The first absorption peak could be ascribed to the π–π^* electron transition within benzenoid segments. The other two absorption peaks at 425 and $>$ 800 nm are attributing to the polaron to π^* electron transition and the π to the localized polaron band, respectively[53]. For the dedoped PANI nanowires, the obvious peak centered at about 670 nm is corresponding to the benzenoid to quinonoid excitonic transition, which is the characteristic band of the dedoped state of the PANI nanowires[53]. As for the MAA doped PANI nanowires, the characteristic peaks of the π–π^* electron transition, polaron-π^* electron transition and π-localized polaron band were observed at 358, 450 and $>$ 800 nm, indicating that PANI nanowires are in doped state. The UV-vis absorption spectrum of PANI/Cu_9S_5 composite nanowires showed the characteristic peaks at about 333 and 630 nm,

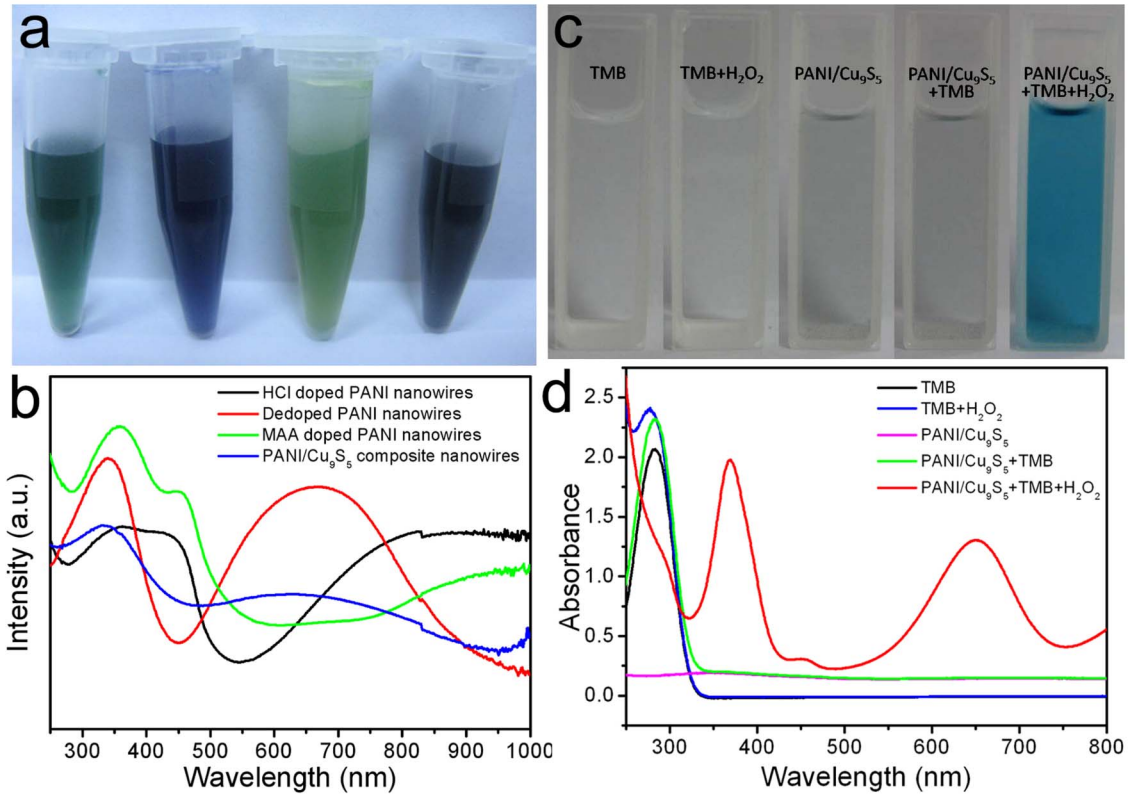

Figure 3 | Absorption spectra property and peroxidase-like catalytic activity of the PANI/Cu_9S_5 composite nanowires. (a) Photographs (from left to right) and (b) UV-vis absorption spectra of aqueous dispersions of HCl doped PANI nanowires (black), dedoped PANI nanowires (red), MAA doped PANI nanowires (green) and PANI/Cu_9S_5 composite nanowires (blue). (c) Photographs (from left to right) and d) UV-vis spectra of TMB solution (black line), TMB-H_2O_2 (blue line), PANI/Cu_9S_5 solution (purple line), PANI/Cu_9S_5 + TMB (green line) and PANI/Cu_9S_5 + TMB + H_2O_2 (red line) in pH 4.0 acetate buffer at room temperature ([TMB]: 0.1 mM; [H_2O_2]: 65 mM; [PANI/Cu_9S_5]: 20 μg/mL).

indicating the low doping level of the PANI in the composite nanowires.

It is well known that some transition metal compound nanoparticles such as Fe_3O_4, FeS and CuS process a peroxidase-like activity[14,28,30]. In this study, we evaluated the catalytic activity of the PANI/Cu_9S_5 composite nanowires by using a peroxidase-like catalytic reaction involving the oxidation of a peroxidase substrate TMB in the presence of H_2O_2. Similar to HRP, PANI/Cu_9S_5 composite nanowires could quickly catalyze the oxidation of TMB in the presence of H_2O_2 to produce a typical blue color in only several minutes, showing their good peroxidase-like activity. Control experiments were also performed to demonstrate that the peroxidase-like activity was attributed to the nanocatalysts of PANI/Cu_9S_5 composite nanowires. As shown in Figure 3c, the TMB + H_2O_2 system without PANI/Cu_9S_5 composite nanowires was colorless, and also no blue color was generated for the PANI/Cu_9S_5 composite nanowires + TMB system under experimental conditions. This result suggested that neither H_2O_2 nor PANI/Cu_9S_5 composite nanowires alone could catalyze the oxidation of TMB. UV-vis spectra have also been used to evaluate the peroxidase-like activity of PANI/Cu_9S_5 composite nanowires (Figure 3d). It was seen that no obvious adsorption peaks ranging from 330 to 750 nm were observed for TMB solution, PANI/Cu_9S_5 composite nanowires dispersions, TMB + H_2O_2 system and PANI/Cu_9S_5 composite nanowires + TMB system. However, three strong adsorption peaks centered at 369, 453, and 652 nm appeared for the PANI/Cu_9S_5 composite nanowires + TMB + H_2O_2 system, which originates from the oxidation of TMB. This result revealed that PANI/Cu_9S_5 composite nanowires could catalyze the oxidation of TMB in the presence of H_2O_2. It is well known that Cu^{2+} and Fe^{3+} are common Fenton regents, which could also efficiently catalyze the oxidation of TMB in the presence of H_2O_2. To rule out the possibility that the Cu^{2+} leaching from PANI/Cu_9S_5 composite nanowires act as the catalysts for the oxidation of TMB, we also performed a comparison experiment to test the peroxidase-like activity of the leaching solution. It was found that no obvious change of absorbance was observed when the leaching solution was used as the catalysts under the same reaction conditions (Figure S3). These results suggested that the peroxidase-like activity was due to the PANI/Cu_9S_5 composite nanowires.

Discussion

As comparisons, we have evaluated the peroxidise activity of PANI/Cu_9S_5 composite nanowires, Cu_9S_5 nanocrystals, PANI nanowires and even the physical mixture of Cu_9S_5 nanocrystals and PANI nanowires, respectively. As shown in Figure 4a and b, free PANI nanowires almost showed no catalytic activity, and Cu_9S_5 nanocrystals alone had a low catalytic activity. The physical mixture of Cu_9S_5 nanocrystals and PANI nanowires showed a similar catalytic activity with that of pristine Cu_9S_5 nanocrystals. However, the PANI/Cu_9S_5 composite nanowires exhibited a surprising high activity. The catalytic activity of the PANI/Cu_9S_5 composite nanowires processed a factor of about 30 fold higher than that of Cu_9S_5 nanocrystals and more than 1000 fold excess higher than that of PANI nanowires. The high catalytic activity might be due to the small size of the Cu_9S_5 nanocrystals on the surface of PANI nanowires. And the synergetic coupling effects between PANI nanowires and Cu_9S_5 nanocrystals in the PANI/Cu_9S_5 composite nanowires might also play an important role on mimicking peroxidases. It has been reported that the interfaces is important to achieve a better activity and selectivity during the catalytic reactions[36,37]. Therefore, the synergetic catalytic effect in the composites should be due to the strong contact between PANI

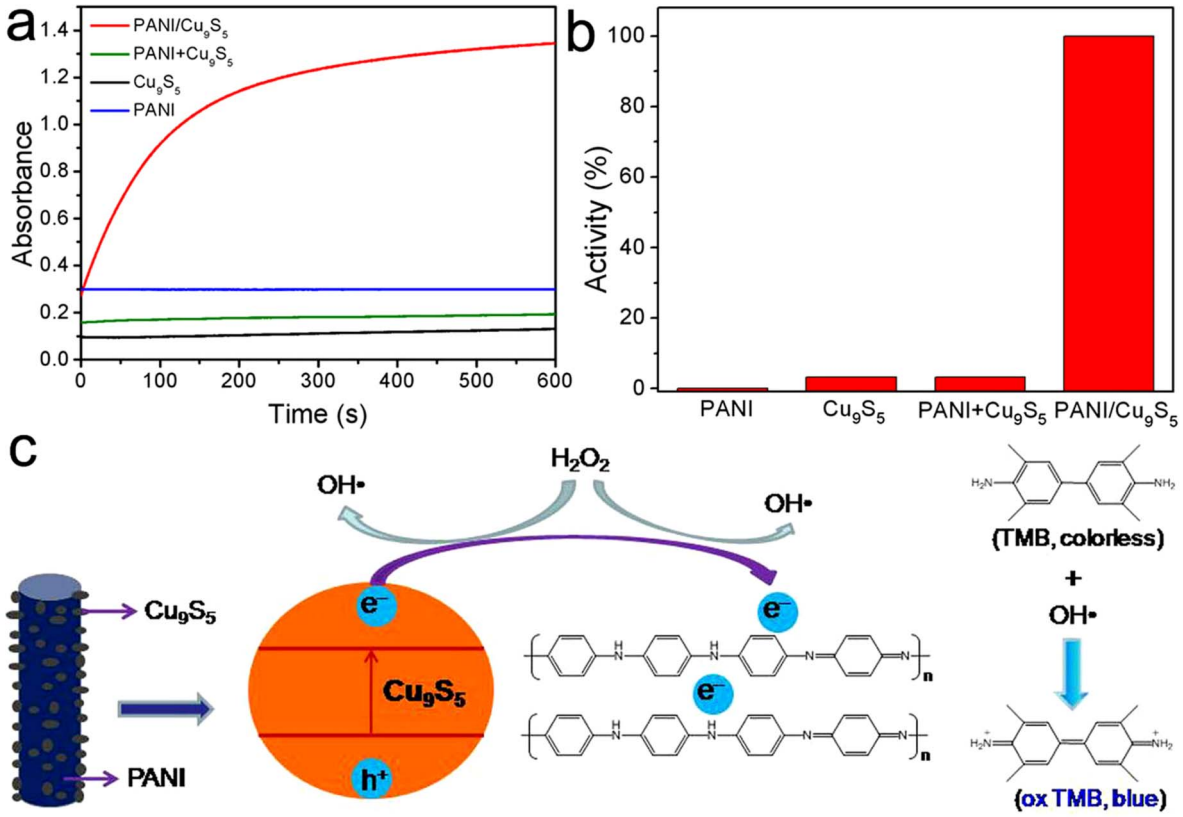

Figure 4 | Synergetic catalytic effect and the mechanism of the PANI/Cu_9S_5 composite nanowires toward the oxidation of TMB. (a) The time-dependent absorbance changes at 652 nm in the presence of pristine Cu_9S_5 nanocrystals, PANI nanowires, the physical mixture of PANI nanowires and Cu_9S_5 nanocrystals, and the as-prepared PANI/Cu_9S_5 composite nanowires in pH 4.0 acetate buffer (0.1 M NaAc-HAc) at room temperature; (b) Comparison of the catalytic activities of PANI nanowires, pristine Cu_9S_5 nanocrystals, the physical mixture of PANI nanowires and Cu_9S_5 nanocrystals, and PANI/Cu_9S_5 composite nanowires under the same conditions. The difference of the absorbance between 10 and 0 min stands for the activity and the maximum point was set as 100%. (c) A possible mechanism of the synergetic catalytic effect of the PANI/Cu_9S_5 composite nanowires toward the oxidation of TMB.

nanowires and Cu_9S_5 nanocrystals. An early report has shown that Au/graphene hybrid with strong covalent interfacing exhibited a synergetic catalytic effect in peroxidase-like catalysis[41]. In this paper, we have synthesized Cu_9S_5 nanocrystals on the surface of PANI nanowires by using the dopant of PANI nanowires as the sulfur source, producing a strong contact between the two nanocomponents, which enhances the catalytic activity for the oxidation of TMB. In order to verify the synergetic catalytic effect between PANI nanowires and Cu_9S_5 nanocrystals, we have also synthesized multi-walled carbon nanotubes (MWCNT)/Cu_9S_5 composite nanotubes using a hydrothermal reaction and studied their catalytic activity toward the oxidation of TMB for mimicking peroxidises. TEM image showed that Cu_9S_5 nanocrystals were well dispersed on the surface of MWCNT nanotubes with a very small size, most of which was in the range of 5–30 nm (Figure S4). However, the as-synthesized MWCNT/Cu_9S_5 composite nanotubes showed a low catalytic activity toward the oxidation of TMB compared with that of PANI/Cu_9S_5 composite nanowires (Figure S5). This result further proved that the synergetic catalytic effect between PANI nanowires and Cu_9S_5 nanocrystals contributed the high catalytic activity of PANI/Cu_9S_5 composite nanowires for the oxidation of TMB.

A possible mechanism for the enhanced catalytic activity of the PANI/Cu_9S_5 composite nanowires toward the oxidation of TMB has been demonstrated. Based on the previous reports, the blue color product should be due to the oxidation of TMB by OH·[54,55]. Cu(II) on the surface of Cu_9S_5 nanocrystals might produce OH· by the Fenton reaction between Cu(II) and H_2O_2[30]. However, this pathway to produce OH· could not explain the enhanced catalytic activity of the PANI/Cu_9S_5 composite nanowires compared to that of Cu_9S_5 nanocrystals. We think that the adsorbed H_2O_2 could also be catalyzed by the PANI/Cu_9S_5 heterostructures. As shown in Figure 4c, when PANI was coupled with a narrow band gap semiconductor such as Cu_9S_5 under visible light irradiation, the photogenerated electrons excited by Cu_9S_5 will transfer from Cu_9S_5 to PANI, which effectively prevent the recombination of the electron-hole pairs. And H_2O_2 is a good electron scavenger to form OH· on the surface of composite nanowires, which largely enhanced the oxidation ability of TMB[55]. As a result, the PANI/Cu_9S_5 composite nanowires exhibited an enhanced catalytic activity compared to the individual Cu_9S_5 nanocrystals and PANI nanowires alone.

In summary, PANI/Cu_9S_5 composite nanowires have been fabricated under a hydrothermal reaction between MAA doped PANI nanowires and copper chloride. This method affords an effective route to decorate Cu_9S_5 nanocrystals on the surface of PANI nanowires with a strong contact. The obtained Cu_9S_5 nanocrystals were well dispersed on the surface of PANI nanowires. The as-synthesized PANI/Cu_9S_5 composite nanowires show a high catalytic activity towards the oxidation of TMB for mimicking peroxidases. The catalytic activity of the PANI/Cu_9S_5 composite nanowires is much higher than that of Cu_9S_5 nanocrystals and PANI nanowires alone. The synergetic catalytic effect should be attributed to the strong interactions between PANI nanowires and Cu_9S_5 nanocrystals. It was expected that the PANI/Cu_9S_5 composite nanowires could have great potential practical applications in catalysis and bioassays.

Methods

Chemicals and materials. Aniline was purchased from Xilong Chemical Co. Ltd and was distilled under reduced pressure before use. MAA was purchased from Aladdin. Copper chloride ($CuCl_2 \cdot 2H_2O$) and TMB were purchased from Sinopharm group chemical reagent Co. Ltd. Other reagents such as ammonium peroxydisulfate (APS), hydrochloric acid (HCl), ammonia solution ($NH_3 \cdot H_2O$), hydrogen peroxide (H_2O_2) and ethanol were of analytical grade and were used as received without purification. Distilled water was used in all experiments.

Preparation of MAA doped PANI nanowires. Firstly, HCl doped PANI nanowires was prepared using a modified rapid-mixing reaction method[56,57]. In a typical procedure, an aqueous solution of 0.3 mL aniline monomer in 10 mL of 1.0 M HCl and another aqueous solution of 0.18 g of ammonium peroxydisulfate in 10 mL of 1.0 M HCl were prepared and mixed rapidly. After shaking for about 30 s, the mixture was left for 2 h. The as-synthesized green precipitate of PANI nanowires doped with HCl was centrifuged and washed with distilled water for at least three times.

For the preparation of dedoped PANI nanowires, the as-synthesized PANI nanowires was dispersed in 1.0 M $NH_3 \cdot H_2O$ and stirred for about 8 h. The green PANI nanowires doped with HCl immediately changed to blue after the addition of $NH_3 \cdot H_2O$. The dedoped PANI nanowires was centrifuged and washed with distilled water for at least two times. For the preparation of PANI nanowires doped with MAA, the obtained dedoped PANI nanowires was then dispersed into a MAA solution for about 12 h. Then the MAA doped PANI nanowires was centrifuged and washed with distilled water. Finally, the MAA doped PANI nanowires were dispersed in water for use.

Preparation of PANI/Cu_9S_5 composite nanowires. PANI/Cu_9S_5 composite nanowires were prepared by mixing MAA doped PANI nanowires and $CuCl_2 \cdot 2H_2O$ under a hydrothermal reaction. In a typical procedure, 1 mL of aqueous solution containing 51 mg $CuCl_2 \cdot 2H_2O$ was added into 30 mL of water which containing 15 mg of MAA doped PANI nanowires. After that, the mixed solution was transferred into a 45 mL Teflon-lined stainless steel autoclave at 140°C for 12 h. Finally, the solid product was collected by centrifuge, washing with water and ethanol, and then dried in vacuum at 30°C for one night.

Investigation of the peroxidase-like activity of the PANI/Cu_9S_5 composite nanowires. To evaluate the peroxidase-like activity of the obtained PANI/Cu_9S_5 composite nanowires, the catalytic oxidation of TMB in the presence of H_2O_2 was tested. In a typical experiment, 20 μL of 30% H_2O_2 and 20 μL of 15 mM TMB solution in DMSO solvent (prepared freshly) were added to 0.1 M acetate buffer (pH 4.0). Then, 20 μL of PANI/Cu_9S_5 composite nanowires suspension in water (3.0 mg/mL) was added into the above mixture. The blue color that developed during the process of the reaction was monitored in time by recording the absorption spectra in a scanning kinetics mode.

Characterization. TEM experiments were performed on JEM-1200 EX (JEOL) electron microscopes with an acceleration voltage of 100 kV. HRTEM imaging and energy dispersive X-ray (EDX) analysis were performed on a FEI Tecnai G2 F20 high-resolution transmission electron microscope operating at 200 kV. XRD patterns are obtained with a PANalytical B.V. Empyrean diffractometer using CuKα radiation. FTIR spectra of KBr powder-pressed pellets were recorded on a BRUKER VECTOR 22 Spectrometer. UV-vis spectra were recorded on a Shimadzu UV-3101 and 2501 PC spectrometer. Analysis of the X-ray photoelectron spectra (XPS) was performed on a Thermo Scientific ESCALAB250 measurement.

1. Wulff, G. Enzyme-like catalysis by molecularly imprinted polymers. *Chem. Rev.* **102**, 1–27 (2002).
2. Levine, L. A. & Williams, M. E. Inorganic biomimetic structures. *Curr. Opin. Chem. Biol.* **13**, 669–677 (2009).
3. Kotov, N. A. Inorganic nanoparticles as protein mimics. *Science* **330**, 188–189 (2010).
4. Wang, Q. *et al.* Supramolecular-hydrogel-encapsulated hemin as an artificial. *Angew. Chem. Int. Ed.* **46**, 4285–4289 (2007).
5. Fruk, L. & Niemeyer, C. M. Covalent hemin-DNA adducts for generating a novel class of artifical heme enzymes.*Angew. Chem. Int. Ed.* **44**, 2603–2606 (2005).
6. Aissaoui, H., Bachmann, R., Schweiger, A. & Woggon, W. D. On the origin of the low-spin character of cytochrome P450(cam) in the resting state: investigations of enzyme models with pulse EPR and ENDOR spectroscopy.*Angew. Chem. Int. Ed.* **37**, 2998–3002 (1998).
7. Genfa, Z. & Dasgupta, P. K. Hematin as a peroxidase substitute in hydrogen peroxide determinations. *Anal. Chem.* **64**, 517–522 (1992).
8. Wang, Q. L., Liu, Z. H., Cai, R. X. & Lu, G. X. Highly sensitive determination of hydrogen peroxide with hemoglobin as catalyst. *Chin. J. Anal. Chem.* **30**, 928–931 2002.
9. Liu, Z. H., Cai, R. X., Mao, L. Y., Huang, H. P. & Ma, W. H. Highly sensitive spectrofluorimetric determination of hydrogen peroxide with beta-cyclodextrin-hemin as catalyst. *Analyst* **124**, 173–176 (1999).
10. Sono, M., Roach, M. P., Coulter, E. D. & Dawson, J. H. Heme-containing oxygenases. *Chem. Rev.* **96**, 2841–2887 (1996).
11. Bonarlaw, R. P. & Sanders, J. K. M. Polyol recognition by a steroid-capped porphyrin. Enhancement and modulation of misfit guest binding by added water or methanol. *J. Am. Chem. Soc.* **117**, 259–271 (1995).
12. Ci, Y. X., Zheng, Y. G., Tie, J. K. & Chang, W. B. Chemiluminescence investigation of the interaction of metalloporphyrins with nucleic acids. *Anal. Chim. Acta* **282**, 695–701 (1993).
13. Haruta, M. When gold is not noble: catalysis by nanoparticles. *Chem. Rec.* **3**, 75–87 (2003).
14. Gao, L. Z. *et al.* Intrinsic peroxidase-like activity of ferromagnetic nanoparticles. *Nat. Nanotechnol.* **2**, 577–583 (2007).
15. Wei, H. & Wang, E. Fe_3O_4 magnetic nanoparticles as peroxidase mimetics and their applications in H_2O_2 and glucose detection. *Anal. Chem.* **80**, 2250–2254 (2008).
16. Liu, S., Lu, F., Xing, R. & Zhu, J. J. Structural effects of Fe_3O_4 nanocrystals on peroxidase-like activity. *Chem. Eur. J.* **17**, 620–625 (2011).
17. Mu, J. S., Wang, Y., Zhao, M. & Zhang, L. Intrinsic peroxidase-like activity and catalase-like activity of Co_3O_4 nanoparticles. *Chem. Commun.* **48**, 2540–2542 (2012).
18. Chen, W. *et al.* Peroxidase-like activity of water-soluble cupric oxide nanoparticles and its analytical application for detection of hydrogen peroxide and glucose. *Analyst* **137**, 1706–1712 (2012).
19. Asati, A., Santra, S., Kaittanis, C., Nath, S. & Perez, J. M. Oxidase-like activity of polymer-coated cerium oxide nanoparticles. *Angew. Chem. Int. Ed.* **48**, 2308–2312 (2009).
20. Andre, R. *et al.* V_2O_5 nanowires with an intrinsic restigiou-like activity. *Adv. Funct. Mater.* **21**, 501–509 (2011).
21. Jv, Y., Li, B. X. & Cao, R. Positively-charged gold nanoparticles as peroxidase mimic and their application in hydrogen peroxide and glucose detection. *Chem. Commun.* **46**, 8017–8019 (2010).
22. He, W. *et al.* Design of AgM bimetallic alloy nanostructures (M = Au, Pd, Pt) with tunable morphology and peroxidase-like activity. *Chem. Mater.* **22**, 2988–2994 (2010).
23. Kwon, T., Min, M., Lee, H. & Kim, B. J. Facile preparation of water soluble CuPt nanorods with controlled aspect ratio and study on their catalytic properties in water. *J. Mater. Chem.* **21**, 11956–11960 (2011).
24. He, W. *et al.* Au@Pt nanostructures as oxidase and peroxidase mimetics for use in immunoassays. *Biomaterials* **32**, 1139–1147 (2011).
25. Song, Y., Qu, K., Zhao, C., Ren, J. & Qu, X. Graphene oxide: intrinsic peroxidase catalytic activity and its application to glucose detection. *Adv. Mater.* **22**, 2206–2210 (2010).
26. Song, Y. *et al.* Label-free colorimetric detection of single nucleotide polymorphism by using single-walled carbon nanotube intrinsic peroxidase-like activity. *Chem. Eur. J.* **16**, 3617–3621 (2010).
27. Shi, W. *et al.* Carbon nanodots as peroxidase mimetics and their applications to glucose detection. *Chem. Commun.* **47**, 6695–6697 (2011).
28. Dai, Z., Liu, S., Bao, J. & Ju, H. Nanostructured FeS as a mimic peroxidase for biocatalysis and biosensing. *Chem. Eur. J.* **15**, 4321–4326 (2009).
29. Dutta, A. K. *et al.* Synthesis of FeS and FeSe nanoparticles from a single source precursor: A study of their photocatalytic activity, peroxidase-like behavior, and electrochemical sensing of H_2O_2. *ACS Appl. Mater. Interfaces* **4**, 1919–1927 (2012).
30. He, W. *et al.* Understanding the formation of CuS concave superstructures with peroxidase-like activity. *Nanoscale* **4**, 3501–3506 (2012).
31. Maji, S. K. *et al.* Peroxidase-like behavior, amperometric biosensing of hydrogen peroxide and photocatalytic activity by cadmium sulfide nanoparticles. *J. Mol. Catal. A: Chem.* **358**, 1–9 (2012).
32. Luo, W. *et al.* Ultrasensitive fluorometric determination of hydrogen peroxide and glucose by using multiferroic $BiFeO_3$ nanoparticles as a catalyst. *Talanta* **81**, 901–907 (2010).
33. Shi, W., Zhang, X., He, S. & Huang, Y. $CoFe_2O_4$ magnetic nanoparticles as a peroxidase mimic mediated chemiluminescence for hydrogen peroxide and glucose. *Chem. Commun.* **47**, 10785–10787 (2011).
34. Tian, J., Liu, S., Luo, Y. & Sun, X. Fe(III)-based coordination polymer nanoparticles: peroxidase-like catalytic activity and their application to hydrogen peroxide and glucose detection. *Catal. Sci. Technol.* **2**, 432–436 (2012).
35. Liu, S., Wang, L., Zhai, J., Luo, Y. & Sun, X. Carboxyl functionalized mesoporous polymer: A novel peroxidase-like catalyst for H_2O_2 detection. *Anal. Methods* **3**, 1475–1477 (2011).
36. Zhou, Z., Kooi, S., Flytzani-Stephanopoulos, M. & Saltsburg, H. The Role of the Interface in CO Oxidation on Au/CeO_2 Multilayer Nanotowers. *Adv. Funct. Mater.* **18**, 2801–2807 (2008).
37. Yamada, Y. *et al.* Nanocrystal bilayer for tandem catalysis. *Nat. Chem.* **3**, 372–376 (2011).
38. Guo, Y. *et al.* Hemin-graphene hybrid nanosheets with intrinsic peroxidase-like activity for label-free colorimetric detection of single-nucleotide polymorphism. *ACS Nano* **2**, 1282–1290 (2011).
39. Zuo, X. *et al.* Design of a carbon nanotube/magnetic nanoparticle-based peroxidase-like nanocomplex and its application for highly efficient catalytic oxidation of phenols. *Nano Res.* **2**, 617–623 (2009).
40. Dong, Y. *et al.* Graphene oxide-Fe_3O_4 magnetic nanocomposites with peroxidase-like activity for colorimetric detection of glucose. *Nanoscale* **4**, 3969–3976 (2012).

41. Liu, M., Zhao, H., Chen, S., Yu, H. & Quan, X. Stimuli-responsive peroxidase mimicking at a smart graphene interface. *Chem. Commun.* **48**, 7055–7057 (2012).
42. MacDiarmid, A. G. Synthetic Metals: A novel role for organic polymers. *Angew. Chem. Int. Ed.***40**, 2581–2590 (2001).
43. Li, D., Huang, J. & Kaner, R. B. Polyaniline nanofibers: A unique polymer nanostructure for versatile applications. *Acc. Chem. Res.* **42**, 135–145 (2009).
44. Lu, X., Zhang, W. J., Wang, C., Wen, T. C. & Wei, Y. One-dimensional conducting polymer nanocomposites: Synthesis, properties and applications. *Prog. Polym. Sci.* **36**, 671–712 (2011).
45. Lu, X. *et al.* Preparation and characterization of polyaniline microwires containing CdS nanoparticles. *Chem. Commun.*1522–1523 (2004).
46. Raut, B. T. *et al.* New process for fabrication of polyaniline-CdS nanocomposites: Structural, morphological and optoelectronic investigations. *J. Phys. Chem. Solids* **74**, 236–244 (2013).
47. Ameen, S., Akhtar, M. S., Kim, Y. S. & Shin, H. S. Synthesis and electrochemical impedance properties of CdS nanoparticles decorated polyaniline nanorods. *Chem. Eng. J.* **181–182**, 806–812 (2012).
48. Shan, J. *et al.* Synthesis and characterization of copper sulfide nanocrystallites with low sintering temperatures. *J. Mater. Chem.* **18**, 3200–3208 (2008).
49. Hu, H., Liu, Z., Yang, B., Chen, X. & Qian, Y. Template-mediated growth of Cu_3SnS_4 nanoshell tubes. *J. Cryst. Growth* **294**, 226–234 (2005).
50. Roy, P., Mondal, K. & Srivastava, S. K. Synthesis of twinned CuS nanorods by a simple wet chemical method. *Cryst. Growth Des.* **8**, 1530–1534 (2008).
51. Laffineur, F., Delhalle, J., Guittard, S., Geribaldi, S. & Mekhalif, Z. Mechanically polished copper surfaces modified with n-dodecanethiol and 3-perfluorooctyl-propanethiol. *Colloids Surf. A* **198–200**, 817–827 (2002).
52. Atanasoska, L., Naoi, K. & Smyrl, W. H. XPS studies on conducting polymers: polypyrrole films doped with perchlorate and polymeric anions. *Chem. Mater.* **4**, 988–994 (1992).
53. Stejskal, J., Kratochvil, P. & Radhakrishnan, N. The formation of polyaniline and the UV-vis absorption spectra. *Synth. Met.* **61**, 225–231 (1993).
54. Gao, L., Wu, J. & Gao, D. Enzyme-controlled self-assembly and transformation of nanostructures in a tetramethylbenzidine/horseradish peroxidase/H_2O_2 System. *ACS Nano.* **5**, 6736–6742 (2011).
55. Zhao, M. *et al.* Controlled synthesis of spinel $ZnFe_2O_4$ decorated ZnO heterostructures as peroxidase mimetics for enhanced colorimetric biosensing. *Chem. Commun.* **49**, 7656–7658 (2013).
56. Huang, J. X. & Kaner, R. B. Nanofiber formation in the chemical polymerization of aniline: A mechanistic study. *Angew. Chem. Int. Ed.* **43**, 5817–5821 (2004).
57. Hang, J., Li, L. Y. & Guo, R. Novel approach to controllable synthesis of gold nanoparticles supported on polyaniline nanofibers. *Macromolecules* **43**, 10636–10644 (2010).

Acknowledgments

X.F.L. acknowledges the funding support from the National Natural Science Foundation of China (51273075), Jilin Science and Technology Department project (201115014) and Open Project of State Key Laboratory of Supramolecular Structure and Materials (sklssm201221). C.W. thanks the National Key Technology Research and Development Program (2013BAC01B02) and the National Natural Science Foundation of China (No. 21274052).

Author contributions

X.F.L supervised the project, planned and performed the experiments, collected and analysed the data, and wrote the paper. X.J.B. performed the experiments, collected and analysed the data. Z.C.L. was responsible for TEM measurement and analysis. D.M.C. helped with synthesis of the materials and collected the data. C.W. supervised the project and analysed the data.

Additional information

Supplementary information accompanies this paper at http://www.nature.com/scientificreports

Competing financial interests: The authors declare no competing financial interests.

How to cite this article: Lu, X.-F., Bian, X.-J., Li, Z.-C., Chao, D.-M. & Wang, C. A facile strategy to decorate Cu_9S_5 nanocrystals on polyaniline nanowires and their synergetic catalytic properties. *Sci. Rep.* **3**, 2955; DOI:10.1038/srep02955 (2013).